

Observation of Impact Energy Absorption Performance on Idealised Trabecular forms in Laser Sintered Nylon

John R McCardle, Loughborough Design School, Loughborough University, UK

Joseph Bunyan, Duku Design, Cheltenham, UK

Abstract

Case studies involving the analysis of impact properties of trabecular bone in mammalian skeletons provide evidence for the natural evolution of energy absorbing architecture as the location of trabecular bone seems to occur in areas that can be subject to high impact and stresses and where the arrangement of the individual trabecular is oriented according to mechanical stimulus. Natural trabecular skeletal bone consists of a complex network of interlinking rod-like and/or plate-like structures and is found in varying proportions depending on the anatomical site of natural the skeleton. Designers and engineers may find biomimetic methods of absorbing shock and impact an efficient alternative consideration in design applications.

This study investigated whether the trabecular architecture found in natural bone can be effectively replicated through the Selective Laser Sintering process of Nylon P2200. Trabecular bone was idealised into a scaled up hexagonal cell proven to replicate the natural structure. The structure was modelled in Solidworks 2013 to form a network of interlinking cells. The specific property analysed was the structure toughness through the measurement of the energy absorbed before sample fracture. This work documents original testing of both the RP material and consolidated design of samples of idealised bone structures.

It was found that impact absorption can be increased with the integration of a greater number of trabecular cells producing a finer resolution and not necessarily by increasing the trabecular size. The information gained from this research may be useful in the design of impact and shock absorbing components, with an emphasis on efficient use of material mass. It also provides an insight into the application of laser sintering as an emerging manufacturing technology to control trabecular detail. It builds on previous work in the area and through the results of empirical testing, derives recommendations for further considerations in this area of design and manufacture of biomimetic structures.

Introduction

Evolutionary solutions have received greater attention with a number of studies exploring the energy absorbing capabilities of naturally occurring structures and there is interest in the potential of replicating and integrating natural forms into designs for added efficiency. There is evidence to suggest that there exists natural solutions for impact and shock absorption, particularly where minimal mass is required (McKittrick, 2010) (Wang & Niu, 2013)

This investigation explored idealised forms of naturally occurring structures that have evolved within animal tissue and that have been theorised to aid in shock and impact energy absorption capabilities. Such materials include the spongy dampening architecture found in natural bone.

The purpose of the study was also to provide insight into the capabilities of a current Additive Manufacturing technique, that of Selective Laser Sintering, to manufacture engineered structures that could be effectively used in designs that require lightweight energy absorbing materials. Such examples include crumple zone panelling for transport, sports protection equipment, and safety wear such as bicycle helmets.

There are two types of bone in anatomy, cortical bone, and trabecular bone, which together comprise the entire skeleton (Trabecular Bone, 2014). The two varieties of bone coexist within individual bones. Cortical bone is compact in nature, with a high level of mineralised content, and is located at the outer surface. Beneath this is a complex bone network, slightly spongy in nature, known as trabecular, cancellous or spongy bone (An & Draughn, 2000). Trabecular bone is significantly less dense than cortical bone, due to its porous structure composed of interconnecting rods and plates (McKittrick, 2010). Comparatively, the porosity of cortical bone and trabecular bone is approximately 5-10% and 50-90% respectively (Trabecular Bone, 2014). Trabecular bone is located in areas of the skeleton where resistance to high impact loads is important, which evolutionists suggest has naturally evolved to as an impact and shock absorbing function. Examples of this include the ends of long bones, such as the mammalian femur, and extending to other species, the impact absorbing skull of a woodpecker (Wang & Cheung, 2011).

Evidence supporting the impact absorbing capabilities of trabecular bone has been reviewed in terms of location within the skeletal structure and the arrangement of the bones. These capabilities of trabecular bone focuses on a structural material providing two key biomechanical roles:

1. Bones protect vital organs from trauma.
 - An example of this is in the skull, mechanical energy from an impact or force concentrates mainly on the spongy bone between an outer and inner plate. As a result, very little energy is transferred to the inner plate, and hence the cranial vault.
2. Distribution of forces due to bone geometry.
 - The ends of bones are broadened; therefore stress is distributed widely across the trabecular bone beneath the outer surface.

Every bone will typically contain some portion of trabecular architecture; however large volumes exist in more localised regions of the skeleton. In the human skeleton, trabecular bone is found at the ends of the long bones and in the vertebral bodies. An example of this has already been illustrated at the end of the proximal femur. The amount of trabecular bone located adjacent to joints would suggest that it plays a large role in maintaining their structural integrity, through absorbing impact and distributing load. It appears that mammalian skeletons have optimized their bones to provide this protection with minimal mass (Parkinson & Fazzalari, 2012).

Trabecular bone itself can be categorised into two groups; rod-like trabecular and plate-like trabecular (Wang & Cheung, 2011), however four types of trabecular bone have been identified (Singh, 1978), which exhibit differences with rod-like and/or plate-like architecture. Although Singh has defined these various structure types, there is little comment on the effective impact absorption capability of each one.

The porous nature of trabecular bone provides a volume for bone marrow, and is hence responsible for blood cell production (Trabecular Bone, 2014), yet it is acknowledged that the spongy, semi flexible properties of this bone construction do serve a mechanical function (Evans, 1973), and the porous volumes provide an area for deformation. The individual trabecular show a defined directional orientation (Singh, 1978), an example of this is the human femur which are subject to bending moments with tensile and compressive stresses.

In summary, there is significant evidence suggesting the impact absorbing purpose and capabilities of trabecular bone. This is supported by considering the trabecular bone location and orientation, particularly in areas which are subject to environmental load, impacts and stresses, such as those experiences at the ends of long bones, and the sandwich layers reinforcing the skull. Considering the large differences in impact absorbing capabilities observed suggests that the structure and geometry of trabecular bone can be largely attributed to its shock absorbing success.

Idealising trabecular structures for manufacture

Geometrically trabecular bone is comprised of a continuous 3-dimensional network of rod-like and/or plate-like individual trabecular of various sizes and orientations, depending on the anatomical site (Kadir, 2010). The four categories of trabecular structure identified by Singh (1978) are based largely on the orientation of the individual elements and whether they are comprised of majority rod-like or plate-like architecture.

There is significant interest in replicating and simulating the trabecular architecture for medical purposes such as bone grafts and implants (Bibb & Sias, 2002). Reconstructing the actual geometry of trabecular bone is difficult due to its complex and highly variable nature (Kadir, 2010) although some complex algorithms have been attempted (Sias et al, 2002). In response to these limitations, idealised structures have been developed which are recognised widely as sharing similar structural properties to natural trabecular architecture (Kadir & Syahrom, 2009). In studies reviewing geometries, Kadir (*ibid.*) has idealised the trabecular structure into three 3-dimensional forms; the hexagonal, the prismatic and the quadratic. These have been further categorised into those structures containing only rod-like architecture, and those incorporating plate-like as well as rod-like structures (Kadir, 2008). The hexagonal architecture has been identified as having closest resemblance to natural trabecular bone.

Kadir further recorded measurements of the key indices required to mimic the 3 dimensional structures. Trabecular thickness ranged between 0.084mm up to 1.89mm, with a mean thickness of 0.366mm. Average bone volume fraction was 0.322, equating to a porosity of approximately 70% (Kadir, 2008). This research into mechanical properties and geometries assumed the bone structure to be homogenous, isotropic and linearly elastic.

Methodology

It is the impact absorption capabilities of the trabecular architecture that was the focus of this study. Its aim was to provide some insight into the potential for the trabecular architecture found in natural bone to be emulated in synthetic samples of laser sintered nylon (PA 2200). Selective Laser Sintering (SLS) provided an opportunity of manufacturing stronger samples with finer detail. As it is ideal for producing complex and accurate forms there was less likelihood of stress raisers being produced as

would be evident in a lower resolution striated AM process. The mechanical properties of the Nylon material used in manufacturing the samples are provided in table 1.


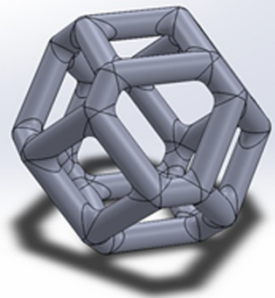
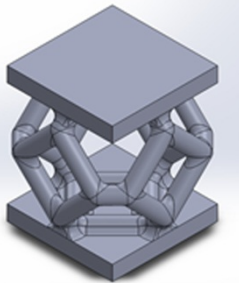
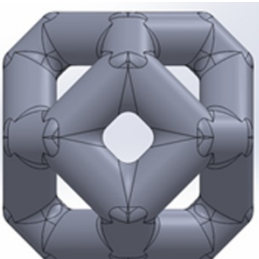
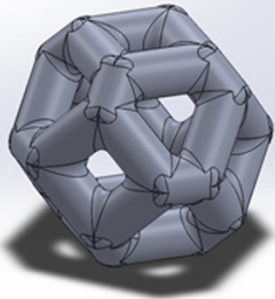
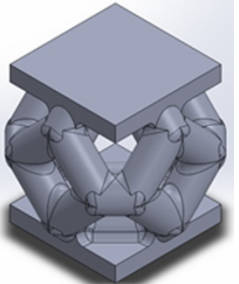
Table 1: Nylon P2200 Data

Mechanical Property	Value	Units	Standard
Flexural modulus (23°C)	1500	Mpa	ISO 178
Izod Impact notched (23°C)	4.4	kJ/m ²	ISO 180/1A
Shore D hardness (15s)	75		ISO 868
3D Mechanical Data			
Tensile Modulus (X Direction)	1650	MPa	ISO 527-1/-2
Tensile Modulus (Y Direction)	1650	MPa	ISO 527-1/-2
Tensile Modulus (Z Direction)	1650	MPa	ISO 527-1/-2
Tensile Strength (X Direction)	48	MPa	ISO 527-1/-2
Tensile Strength (Y Direction)	48	MPa	ISO 527-1/-2
Tensile Strength (Z Direction)	42	MPa	ISO 527-1/-2
Strain at Break (X Direction)	18	%	ISO 527-1/-2
Strain at Break (Y Direction)	18	%	ISO 527-1/-2
Strain at Break (Z Direction)	4	%	ISO 527-1/-2
Charpy impact strength (+23°C, X Direction) (+23°C)	53	kJ/m ²	ISO 179/1eU
Charpy notched impact strength (+23°C, X Direction) (+23°C)	4.8	kJ/m ²	ISO 179/1eU

Solidworks 2013 3D modelling software was used to reproduce the 3D hexagonal structure. Two trabecular cell samples were modelled, both with exactly the same skeleton. The trabecular thickness formed the difference between the two, which affected the bone volume fraction and the trabecular separation. Each cell was bounded by a top and bottom plate 1mm in thickness. The structures are detailed in table 2.

Individual trabecular are typically 100µm in thickness at their thinnest point (McKittrick, 2010), although previous research has found them to exist up to 2.0mm in thickness as well (Singh, 1978), which is feasible to produce from an additive manufacturing perspective. Although additive manufacture has the potential to print on a scale of 10µm, the minimum feature thickness recommended is 1mm (Bingham, 2013), which informed the selected thicknesses in this instance.

Table 2: Two idealised trabecular bone cells replicated in Solidworks 2013

	Side View	$\frac{3}{4}$ Perspective	Isometric
Structure 1 – 1mmØ trabecular			
Structure 2 – 1.5mmØ trabecular			

Tables 3 and 4 illustrate the cross sections of the four material samples. Samples 1a and 1b are solid homogenous material, whereas 2a and 2b feature the trabecular architecture between an inner and outer plate of 1mm thickness. The X and Y geometry of all of the samples was constant, and equated to 54.5 x 59mm. The only variable between group samples 1 and 2 was the inclusion or exclusion of the internal trabecular architecture. The build material was the same for all samples (SLS Nylon – PA 2200).

Sample 1a measured 2mm in thickness. This was the combined thickness of the solid inner and outer plate sandwiching the trabecular architecture on samples 2a and 2b. Sample 1b was 9mm in thickness, which was the total Z axis thickness of samples 2a and 2b, including the trabecular architecture. Solid samples 1a and 1b were produced so that the effect of the trabecular architecture could be compared directly to a solid material. Trabecular bone is known to maximise efficiency with minimal mass. By comparing samples 2a and 2b with both 1a and 1b, mass efficiency was also analysed with respect to bone volume fraction. BV/TV (bone volume fraction) was as indicated in Table 3. A BV/TV value of 100% for sample 1b equated to a solid volume of 54.5 x 59 x 9mm. The values for the samples 1a, 2a and 2b were calculated with respect to this upper limit volume.

Table 3: Sample Design

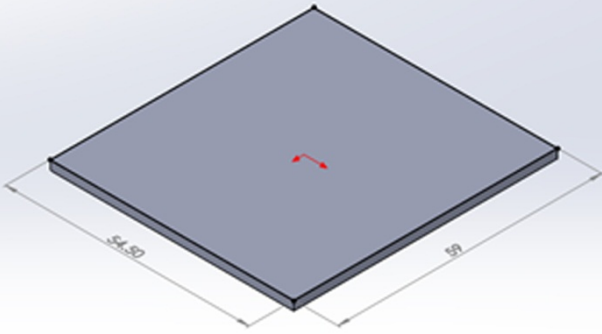

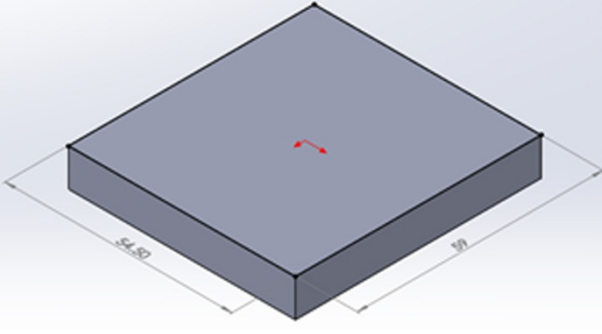

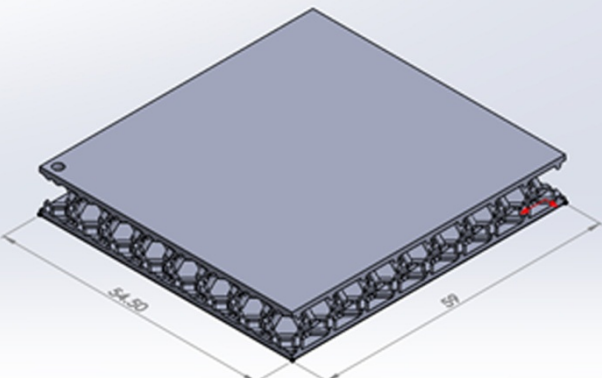
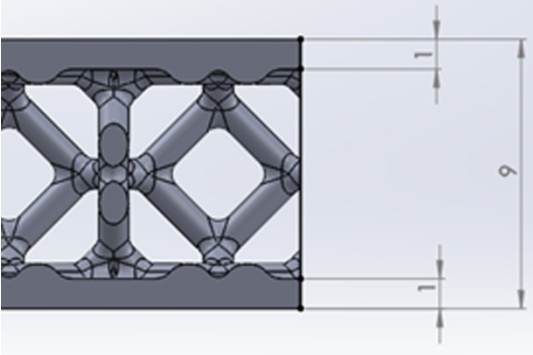
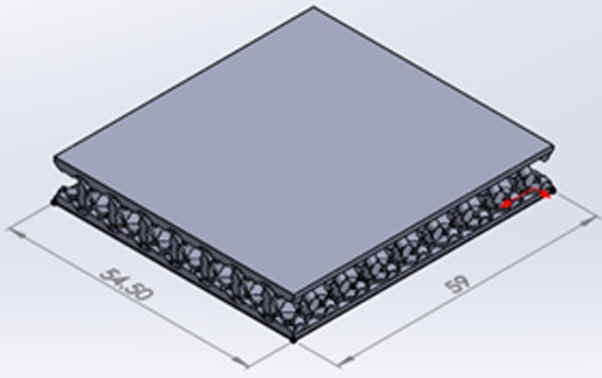
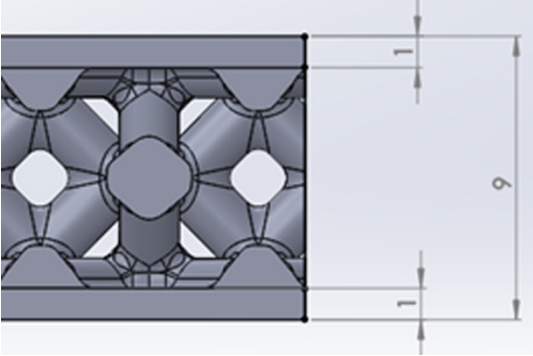








Sample	Isometric	Side View
1a		
1b		
2a		
2b		

Table 4: Test sample Details

#	Side cross sectional view	Z (mm)	outer plate (mm)	Trabecular (Tb.Th) (mm)	(BV/TV) (%)	Porosity (%)	S PA 22 00
1 a		2	-	-	22	0	1 x SL S
							
1 b		9	-	-	100	0	1 x SL S
							
2 a		9	1	1.0	11.9	88.1	6 x SL S
							
2 b		9	1	1.5	34.0	66.0	6 x SL S
							

Mechanical Test

A Falling Dart Drop Impact Test was carried out on all samples using the Rosand Impact Tester. The machine uses a very low clamp force to prevent any damage to the internal trabecular architecture. The mass and dart is raised to the specified height of 0.5m, and is released to freefall, allowing the pre-set 20mmØ flat dart to puncture the sample.

Set-up conditions were as shown in table 5.

Table 5: Setup Test Details

Criteria	Value	Units
Ambient temperature	23	°C
Drop mass	10	kg
Drop Height	0.5	m
Velocity	3.13	m/s
Kinetic Energy	50	J
Recorded		
Peak force		N
Peak energy		J
Total Energy at failure		J
Test duration		s

Results & Analysis

Figure 1 shows a comparison between the force output of both sample groups 2a and 2b. There are distinct differences in the failure effect of both structures. Group 2b exhibited a steep, linear gradient, representing a short and direct deceleration before peak force output/material fracture. The average time before peak force/fracture was 1.09 milliseconds, as opposed to 3.59 milliseconds for group 2a. The linear nature of the 2b curve represents a constant failure rate. The 1.5mm \emptyset trabecular architecture did not provide significant extended periods of deceleration through absorbing energy.

Group 2a showed very different result. The curve had a much lower gradient, and featured an extended period of deceleration, averaging 3.59 milliseconds before peak force/fracture. The staggered nature of the curve represents the buckling of the individual trabecular before fully fracturing the sample. This extended the deceleration period, and hence increased the energy absorbed during fracture. This action may be seen as similar to the sponge-like properties observed in nature, such as that found by (Wang & Niu, 2013).

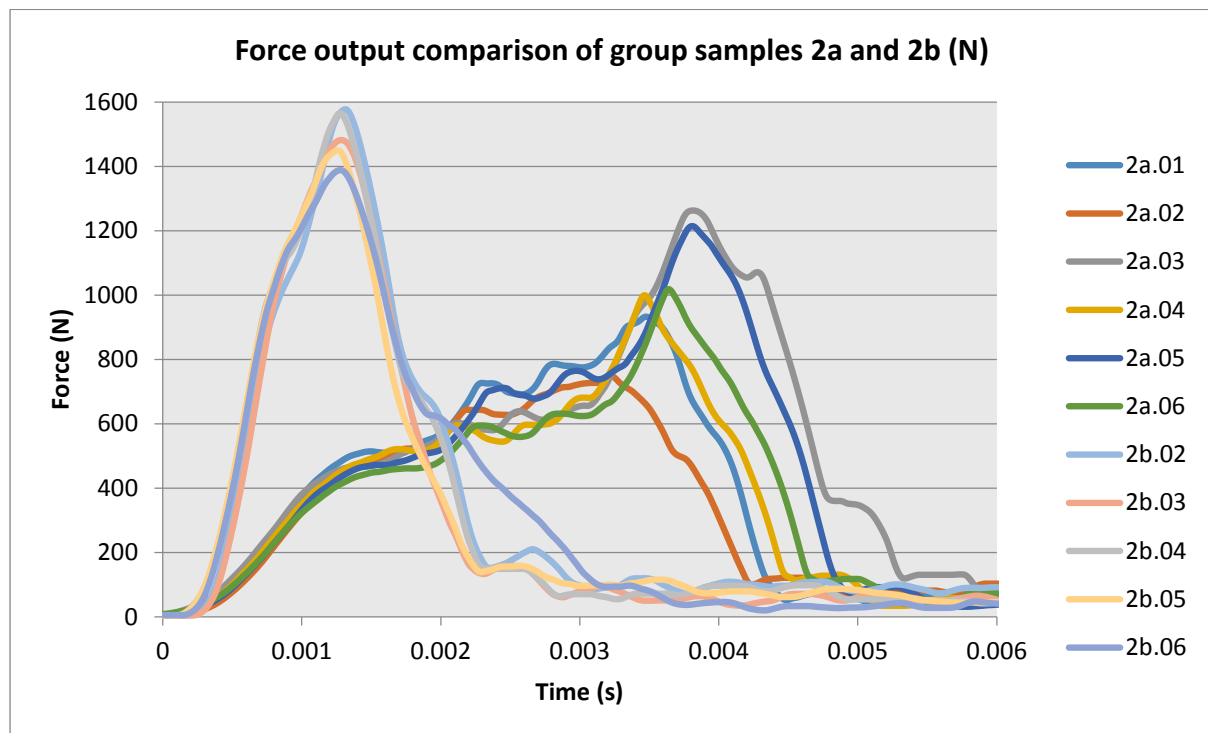


Figure 1: Force output comparison of group samples 2a and 2b

The differences can, in part, be attributed to the change in trabecular thickness. The network of 1.0mm rods in group 2a being weaker than the inner and outer 1mm plates, allowing for elastic deformation. As a result, these would tend to buckle at a lower force, as indicated by the transience in figure 3.

Group 2b, with a network of 1.5mm thick trabecular, required a higher force to fracture, however the act of fracturing was indicated as being much more instantaneous. The trabecular architecture does not seem to offer the same spongy characteristic, because the geometry is thicker than the inner and outer plates. This has resulted in a 'blow out' failure mode, with a rapid deceleration, reducing the materials total energy to fracture, and hence its impact absorbing capabilities.

Figure 2 shows the graphical comparison of force output for all four samples tested. As expected, sample 1b absorbed the greatest amount of energy, and did not feature a break under the test conditions. Following this, sample 1a absorbed the second highest value of energy, followed by sample 2a.Avg and 2b.Avg.

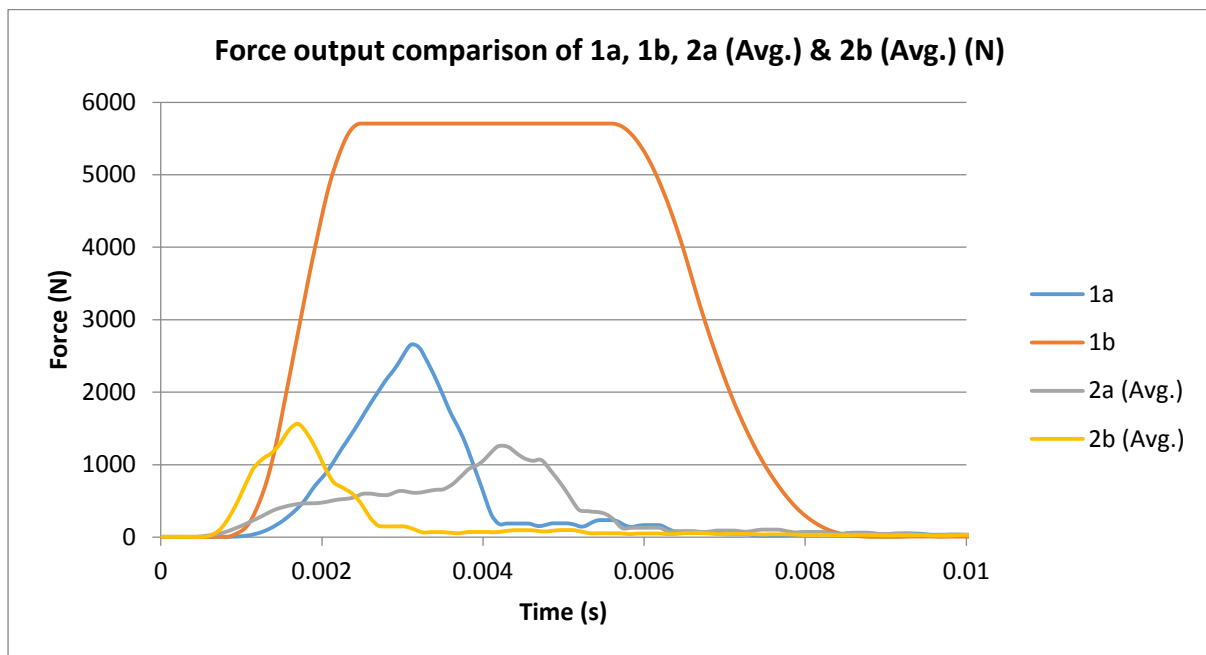


Figure 2: Force output comparison of 1a, 1b, 2a (Avg.) & 2b (Avg.) (N)

Table 6: Comparison of sample properties with average test results

Sample Group	Z dimension (mm)	outer plate thickness (mm)	Trabecular thickness (Tb.Th) (mm)	Bone volume fraction (BV/TV) (%)	Porosity (%)	Avg. Peak Force (N)	Avg. Peak Energy (J)	Avg. Peak Energy time ($\times 10^{-3}$ s)	Avg. Total Energy (J)
1a	2	-	-	22	0	2.66 kN	6.74	3.12	12.7
1b	9	-	-	100	0	5.71 kN	12.53	1.94	49.59
2a Avg.	9	1	1.0	31.5	88.1	1.03 kN	5.18	3.56	7.34
2b Avg.	9	1	1.5	48.7	66.0	1.48 kN	2.59	1.09	5.37

Bones are known to grow in a way to maximise mechanical function whilst minimising mass. With respect to this test, this equates to minimising the volume of material (BV/TV) whilst maintaining impact absorbing properties. In natural bone this is characterised as Bone Mineral Density (BMD) (Ulrich et al, 1999), not a property of the bone materials itself but as a measure of porosity. Indeed in natural trabecular bone while there is postulated that there is a correlation between the BV/TV variance of elasticity, there is a lack of explanation for the mechanical properties due to overall architecture (*ibid*). The results can be compared in table 6 to analyse the efficiency of the volume of material in absorbing energy. Sample 1b featured a no break, making it difficult to analyse this sample other than stating that it included the greatest quantity of material and experienced the highest value of energy absorption. The BV/TV value for samples 1a, 2a and 2b has been calculated as a percentage of the total volume of sample 1b (which included the uppermost volume of material). Sample 1a absorbed a total of 12.7 Joules of energy with a BV/TV value of 22% of that of 1b. Sample 2a featured a BV/TV of 31.5, 30% higher than that of sample 1a, however experienced a total energy absorption value of 7.34 Joules, which is 42% lower than that of sample 1a. This shows that despite an increase in BV/TV percentage for sample 2a over sample 1a, there was still a drop in energy absorption percentage. However, sample 2a did feature an extended period of deceleration. Sample 2b featured a BV/TV value of 48.7, 54.8% higher than sample 1a, and 35.3% higher than sample 2a. Its total energy absorbed was 5.37 J, 57.7% lower than sample 1a and 26.8% lower than sample 2a. Despite a higher BV/TV value of sample 2b compared to both samples 1a and 2a, the total energy absorbed by the sample still fell. For this reason, the trabecular material in sample 2b offers little functional purpose. The increase in the time to reach peak energy prevents similar conclusions for sample 2a.

It was found that the peak and total energy required was greatest for the solid samples excluding the internal trabecular architecture. The values for those samples including the trabecular architecture did show promise, particularly those incorporating the 1.0mm hexagonal trabecular architecture. However the 1.5mm thick trabecular offered little improvement to impact absorption.

The process of additive manufacturing these samples, in this case SLS, would have produced characteristics which would be more detrimental to the structural integrity of samples 2a and 2b compared to the solid samples 1a and 1b. Additive manufacture functions by splitting the component up into layers, which are built upon each other in the z axis which affects impact resistance (Bingham, 2013). This layering technique results in a 'stepping' of the material, exposing weak points in the structure. With the current facilities, these weaknesses are inevitable, and are a

result of the material not being under pressure during processing. The stepping can potentially create micro-scale crack propagation sites between each layer of fused material. Each sample has been built in the same orientation, ensuring the layers are perpendicular to the direction of impact in order to minimise their influence. Due to the fragile and complex structure of the idealised trabecular architecture, which orientates all of its rods at an angle offset from the direction of force, this stepping will have a greater detrimental effect on samples 2a and 2b than 1a and 1b. This proved difficult to specifically quantify, but was noted for future investigation.

Conclusions & Further Research

Despite a lower energy absorption the greatest potential in mimicking the failure mode and impact absorbing properties of natural trabecular was provided by samples that exhibited buckling and deformation of the individual trabecular prior to complete sample failure. This buckling absorbs energy and increases the period of deceleration, a point that may be important for the design of safety and protective equipment.

It is recommended that with the integration of a more complex network of many layers of trabecular architecture, the impact absorbing capabilities may be improved further. As a recommendation, the trabecular architecture could be designed so as to be weaker than the bounding surfaces, ensuring that the individual trabecular experience failure first, maximising their energy absorbing capability through increasing the period of deceleration. The simplest way of doing this is to ensure the rod thickness is less than the bounding material thickness.

Additive manufacturing techniques that have a high resolution deposition, such as SLS, can be used to engineer the trabecular architecture in response to the requirements of a non homogenised an anisotropic forms. Current materials that are used in high impact energy dissipation applications, such as crumple zone materials in transport and safety equipment for sport, often use inexpensive foams which are manufactured from homogenised materials. Such foam structures while maintaining a relatively consistent porosity and density offer little opportunity to manufacture strategically for specific concentrations of potential impact.

In natural bone, impact absorption and energy dissipation may also be influenced by the semi-hydraulic action within the structure due to the red marrow evident in cancellous (trabecular) bone. While this inevitably adds to the mass of bones, as a point of speculation the strength to weight ratio of such a composite structure could still provide additional advantages over dry forms.

References

- An, Y. H. & Draughn, R. A., (2000). *Mechanical Testing of Bone and the Bone-Implant Interface*. 1st ed. New York: CRC Press.
- Bibb, R., Sias, G., (2002), "Bone structure models using stereolithography: a technical note", *Rapid Prototyping Journal*, Vol. 8 Iss 1 pp. 25 - 29
- Bingham, G., (2013), Additive manufactured textiles for high-performance stab resistant applications. *Rapid Prototyping Journal*, 19 (3), pp. 199-207.
- Evans, G., (1973), *Mechanical properties of bone*. 1st ed. Springfield: Charles C Thomas.
- Kadir, A., (2008), Micro-modelling and analysis of actual and idealised cancellous structure. *Biomed*, Volume 21, pp. 433-437.
- Kadir, M. R. A., (2010), Finite element analysis of idealised unit cell cancellous structure based on morphological indices of cancellous bone. *Medical & Biological Engineering & Computing*, 48(5), pp. 497-505.
- Kadir, M. R. A. & Syahrom, A., (2009), Comparison of Permeability on the Actual and Ideal Cancellous Bone Microstructure. *CFD Letters*, 1(2), pp. 68-77.
- McKittrick, J., (2010), *Materials Science and Engineering C. Energy absorbent natural materials and bioinspired design strategies: A review*, C(30), pp. 331-342.
- Parkinson, I. H. & Fazzalari, N. L., (2012), *Characterisation of Trabecular Bone Structure*. *Stud Mechanobiol Tissue Eng Biomater (2013) 5: 31–51* 31, DOI: 10.1007/8415 2011 113, Springer-Verlag Berlin Heidelberg 2012, Published Online: 12 January 2012. [Accessed 20 March 2014].
- Singh, I., (1978), The architecture of cancellous bone. *Journal of Anatomy*, 112(127), pp. 305-310.
- Sias, G., Phillips, R., Dobson, C.A., Fagan, M.J., Langton, C.M., (2002), "Algorithms for accurate rapid prototyping replication of cancellous bone voxel maps", *Rapid Prototyping Journal*, Vol. 8 Iss 1 pp. 6 - 24
- Trabecular Bone, (2014), *mechanical Properties of Trabecular Bone*. [Online] Available at: <http://www.trabecularbone.org/> [Accessed 22 March 2014].
- Ulrich, D., Van Rietbergen, B., Laib, a., & Ruegsegger, P. (1999). The ability of three-dimensional structural indices to reflect mechanical aspects of trabecular bone. *Bone*, 25(1), 55–60. doi:10.1016/S8756-3282(99)00098-8
- Wang, L. & Cheung, J., (2011), Why do Woodpeckers resist head impact injury: A biomechanical investigation. *PlosOne.org*
- Wang, L. & Niu, X., (2013), *Journal of Nanomaterials. Effect of Microstructure of Spongy Bone in Different Parts of Woodpecker's Skull on Resistance to Impact Injury*, 2013(924564), pp. 1-6.